J|A|C|S
ARTICLES
Published on Web 06/10/2006

Magnetic Spin Effects in Enzymatic Reactions: Radical Oxidation of NADH by Horseradish Peroxidase

Maria S. Afanasyeva,[†] Marc B. Taraban,*[,†] Peter A. Purtov,[†]
Tatyana V. Leshina,[†] and Charles B. Grissom*[,‡]

Contribution from the Institute of Chemical Kinetics and Combustion, Novosibirsk-90, 630090 Russia, and the Department of Chemistry, University of Utah, 315 South 1400 East, Salt Lake City, Utah 84112-0850

Received December 19, 2005; E-mail: grissomc@chem.utah.edu; taraban@kinetics.nsc.ru

Abstract: A description of the elementary steps of the horseradish peroxidase (HRP)-catalyzed oxidation of NADH is presented, along with a quantitative analysis of the magnetic-field dependence of the enzymatic reaction. In the absence of H_2O_2, the catalytic cycle begins with single-electron transfer from NADH to native HRP to form the $NADH^{\bullet+}$ radical cation and the ferroperoxidase intermediate (Per^{2+}). The theoretical framework for the magnetic-field dependent recombination of radical pairs has been extended to describe the magnetic-field dependence of reaction rate constants for multi-spin paramagnetic pairs, including the $NADH^{\bullet+}$ radical cation and Per^{2+} that exist in a correlated quartet electronic spin state. Good agreement between the experimentally observed and the theoretically calculated magnetic-field dependences of the effective rate constants underlines the importance of the initial single-electron-transfer step and supports a model in which the catalytic cycle begins with the one-electron reduction of HRP by NADH.

Introduction

The enzymatic interconversion of NAD^+ and NADH most commonly occurs by hydride transfer, in which one proton and two electrons are transferred synchronously between the C-4 carbon of the nicotinamide ring and an organic substrate molecule.[1] The hydride transfer mechanism is supported by an abundance of evidence, including the high-fidelity of stereochemical transfer at the C-4 carbon of nicotinamide[2] and the lack of hydrogen exchange with water (to greater than 1 part in 10^{17}).[3] Additional evidence in support of hydride transfer as being the dominant reaction pathway for the interconversion of NAD^+ and NADH comes from kinetic isotope effect studies on a variety of nicotinamide-linked dehydrogenases[4] and the quantitative agreement of experimental kinetic and thermodynamic parameters with theoretical descriptions of the hydride transfer mechanism.[5] In contrast, a one-electron pathway for NADH oxidation dominates in photochemically initiated reactions in which an electron from the reduced nicotinamide ring is promoted to a higher-energy molecular orbital. In this case, single-electron transfer generates the $NADH^{+\bullet}$ radical cation, followed by asynchronous transfer of the proton and the second electron in an ECE-type process.[6,7] The asynchronous electron transfer mechanism appears to predominate only when NADH is photochemically activated to a higher-energy reductant such that $E^{\circ\prime} > 320$ mV. The asynchronous ECE-type mechanism should also be kinetically and thermodynamically viable if the electron acceptor strongly favors one-electron transfer.

The oxidation of NADH by horseradish peroxidase (HRP) appears to be one such reaction, in which H_2O_2 oxidizes HRP to form Compound I (Comp I), which is spectroscopically distinct Fe^{IV} and the porphyrin π-cation radical. Compound I is a highly reactive species that can accept a lone-pair electron from various phenolates and enolates to reduce the porphyrin π-cation radical and generate Compound II (Comp II). Because Comp I is a highly oxidized species with a large and positive $E^{\circ\prime}$ value, it can also accept one electron from NADH to form the $NADH^{+\bullet}$ radical cation. This species can undergo deprotonation to yield $NAD^{\bullet}$ and Comp II in a process that is competitive with reverse electron transfer to regenerate NADH and Comp I, as shown by the observation of chemically-induced dynamic nuclear polarization (CIDNP) of one of the C-4 protons in the ^1H NMR spectrum of NADH in the presence of HRP.[8] The catalytic mechanism of HRP is of special interest because of its similarity to other heme-containing enzymes, including the cytochrome P-450 enzyme family and cytochrome C-oxidase.[9,10]

[†] Institute of Chemical Kinetics and Combustion.
[‡] University of Utah.

(1) Carlson, B. W.; Miller, L. L. *J. Am. Chem. Soc.* **1985**, *107*, 479−485.
(2) You, K. *Methods Enzymol.* **1982**, *87*, 101−126.
(3) LaReau, R. D.; Anderson, V. E. *J. Biol. Chem.* **1989**, *264*, 15338−15343.
(4) Powell, M. F.; Bruice, T. C. *J. Am. Chem. Soc.* **1983**, *105*, 7139−7149.
(5) (a) Cheng, J.-P.; Lu, Y.; Zhu, X.; Mu, L. *J. Org. Chem.* **1998**, *63*, 6108−6114. (b) Ostoviè, D.; Lee, I. S. H.; Roberts, R. M. G.; Kreevoy, M. M. *J. Org. Chem.* **1985**, *50*, 4206−4211. (c) Kreevoy, M. M.; Ostoviè, D.; Lee, I. S. H.; Binder, D. A.; King, G. W. *J. Am. Chem. Soc.* **1988**, *110*, 524−530.
(6) Grodkowski, J.; Neta, P.; Carlson, B. W.; Miller, L. L. *J. Phys. Chem.* **1983**, *87*, 3135−3138.
(7) Gêbicki, J.; Marcinek, A.; Zielonka, J. *Acc. Chem. Res.* **2004**, *37*, 379−386.
(8) Afanasyeva, M. S.; Taraban, M. B.; Leshina, T. V.; Purtov, P. A.; Grissom, C. B. *Free Radical Biol. Med.* **2006**, submitted for publication.
(9) Dawson, J. H. *Science* **1988**, *240*, 433−439.
(10) Schlichting, I.; Berendzen, J.; Chu, K.; Stock, A. M.; Maves, Sh. A.; Benson, D. K.; Sweet, R. M.; Ringe, D.; Petsko, G. A.; Sligar, S. G. *Science* **2000**, *287*, 1615−1622.

10.1021/ja0585735 CCC: $33.50

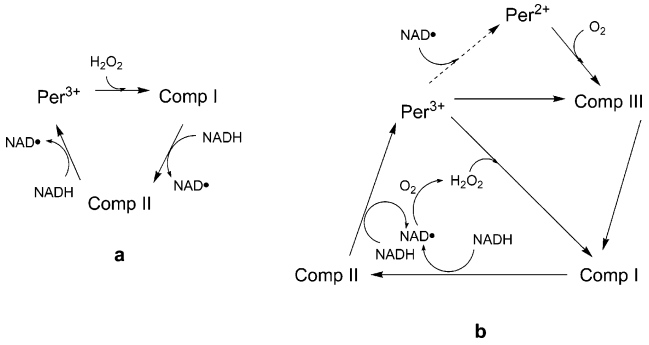

Figure 1. Catalytic cycle of HRP-catalyzed oxidation of NADH: (a) the "simplified form[9]" of the reaction, which exists in the presence of excess H_2O_2; and (b) the "chemically realistic"[12] model. Comp I, II, and III are spectroscopically distinct forms of enzymatically active peroxidase, Per^{3+} is native HRP, and Per^{2+} is the reduced form of HRP or ferroperoxidase.

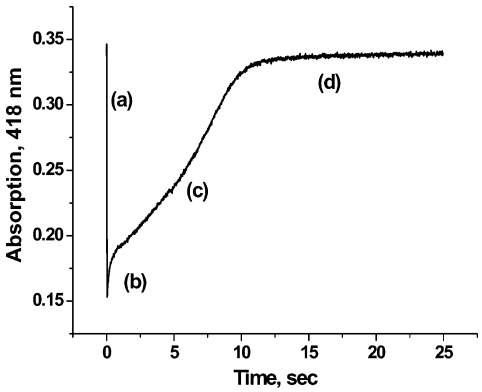

Figure 2. Kinetic trace of chemical transformations observed in HRP-catalyzed oxidation of NADH and digitally extracted at 418 nm. Reaction conditions (all concentrations after mixing): 100 mM MES; pH = 5.56; [HRP] = 1.0 μM; [NADH] = 100 μM; 25.0 °C.

The catalytic cycle of NADH oxidation by HRP in the presence of H_2O_2 begins with a two-electron oxidation of the enzyme to form Fe^{IV} and the porphyrin π-cation radical.[9] The mechanism by which oxidized enzyme is generated is less clear if peroxide is not present, as the catalytic mechanism proposed in Figure 1 is inconsistent with the experimentally observed changes in the concentrations of paramagnetic intermediates.[11] To illustrate the problem, let us compare two commonly accepted mechanisms for NADH oxidation by HRP. The "simplified model"[9] described in Figure 1a begins with the oxidation of HRP by excess H_2O_2,[9] while the "chemically realistic" model (i.e., the absence of excess H_2O_2) described in Figure 1b depends on the uncertain assumption that autoxidation of NADH yields sufficient peroxide to initiate the catalytic cycle.[11,12] The chemically realistic model[12] fails to explain all of the kinetic features observed in the oxidation of NADH in the absence of H_2O_2. Thus, it is unclear what the driving force of NADH oxidation is in the absence of exogenous H_2O_2, what the structures of paramagnetic intermediates in this reaction are, and what the requirements are for electron-spin correlation among the reaction intermediates.

Paramagnetic intermediates in the HRP catalytic cycle and the postulated presence of the NAD• radical are favorable preconditions for the application of electron-spin chemistry techniques[13] to study the elementary steps of the HRP-catalyzed oxidation of NADH. While the direct detection of radicals by EPR depends on trapping a thermodynamically stable paramagnetic intermediate, the magnetic-field dependence of reactions with at least two or more unpaired electrons provides a simplified approach to study kinetically relevant paramagnetic species that may be transient or present only at low concentrations. Furthermore, the magnetic-field dependence of an enzymatic reaction has the potential to reveal electron-spin correlation among the catalytic states of an enzyme. Moreover, the application of electron-spin chemistry techniques to HRP provide clear evidence for single-electron transfer in the oxidation of NADH by the reaction NADH → $NADH^{•+}$ → NAD• → NAD^+.

The magnetic-field dependence of the kinetic rate constants for redox cycling among paramagnetic intermediates in the HRP-catalyzed oxidation of isobutyraldehyde enolate is consistent with the sequential formation of two paramagnetic heme species, Comp I and Comp II, that accept one electron from a diamagnetic electron donor (the isobutryaldehyde enolate) to produce a spin-correlated radical pair.[14] The observed magnetic-field dependence of the peroxidase/oxidase-coupled enzyme oscillator with NADH as electron donor further supports a mechanism in which electron transfer from a diamagnetic electron donor (NADH) to a paramagnetic electron acceptor (Comp I or Comp II) produces a spin-correlated radical pair.[15] Changing the amplitude and timing of the applied magnetic field has even been used to alter the frequency and amplitude of oscillations of O_2 consumption. However, this work was not accompanied by a detailed analysis of the magnetic spin dependence of the HRP-catalyzed oxidation of NADH.

Herein, we report the magnetic-field dependence of single-electron transfer from diamagnetic NADH to the paramagnetic species Comp I and Comp II of HRP. These experiments provide new insight into the initiation steps of the HRP-catalyzed oxidation of NADH in the absence of exogenous H_2O_2. Furthermore, we have expanded the theoretical framework of multi-spin paramagnetic intermediates and the predicted magnetic-field dependence of these electron-spin systems.

Results and Discussion

Stopped-Flow Absorption Spectrophotometry. The oxidation of NADH by HRP in the absence of H_2O_2 was followed by rapid-scanning stopped-flow spectrophotometry, as described previously for the HRP-catalyzed oxidation of 1-(trimethylsilyloxy)-1-propene.[14] A typical stopped-flow absorbance kinetic trace extracted at 418 nm is shown in Figure 2. The plot of absorbance at 418 nm versus time is complex and contains spectral contributions from native HRP, Per^{2+}, Comp I, Comp II, and Comp III. The net change in absorbance versus time at 418 nm can be deconvoluted, as the starting concentration of HRP and the molar absorptivity of each heme chromophore is known[11] (Figure 3). The sharp decrease in absorbance in region *a* of Figure 2 is caused by the formation of the HRP−NADH enzyme−substrate complex, followed by a single-electron-

(11) Yokota, K.; Yamazaki, I. *Biochemistry* **1977**, *16*, 1913−1920.
(12) Scheeline, A.; Olson, D. L.; Williksen, E. P.; Horras, G. A.; Klein, M. L.; Larter, R. *Chem. Rev.* **1997**, *97*, 739−756.
(13) Salikhov, K. M.; Molin, Y. N.; Sagdeev, R. Z.; Buchachenko, A. L. *Spin Polarization and Magnetic Effects in Radical Reactions*; Elsevier: Amsterdam, 1984.
(14) Taraban, M. B.; Leshina, T. V.; Anderson, M. A.; Grissom, C. B. *J. Am. Chem. Soc.* **1997**, *119*, 5768−5769.
(15) Møller, A. C.; Lunding, A.; Olsen, L. F. *Phys. Chem. Chem. Phys.* **2000**, *2*, 3443−3446.

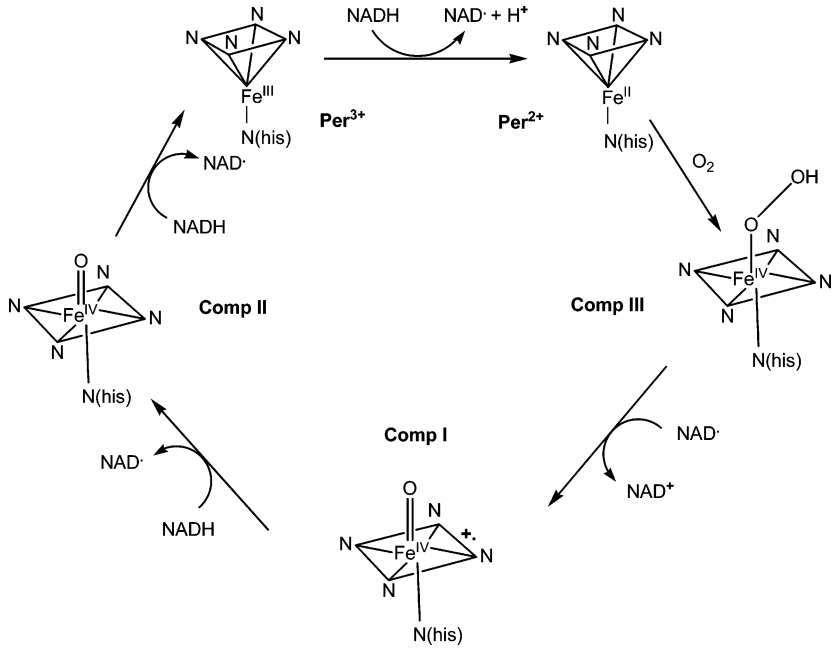

Figure 3. Catalytic cycle HRP-catalyzed NADH oxidation in the absence of H_2O_2.

transfer step. In this process, NADH donates an electron to native HRP, which then becomes ferroperoxidase, Per^{2+} (ϵ = 62 mM^{-1} cm^{-1}) at 418 nm[11] with a lower molar absorptivity than native HRP (ϵ = 102 mM^{-1} cm^{-1}). It is worth noting that the formation of ferroperoxidase, Per^{2+}, was previously thought to be a side reaction of native HRP with intermediate radical species,[11,12] while the scheme presented herein (Figure 3) treats this as an obligate initial step of the catalytic cycle in the absence of H_2O_2. The reaction of ferroperoxidase with dissolved oxygen (Figure 3) rapidly[12] converts Per^{2+} to Comp III (ϵ = 115 mM^{-1} cm^{-1} at 418 nm; $k = 5.8 \times 10^4$ M^{-1} sec^{-1}), thus producing a rapid increase in absorbance (region *b* of Figure 2). Deprotonation of the $NADH^{\bullet+}$ radical cation that is formed in the initial single-electron-transfer step ($k = 3.6 \times 10^6$ sec^{-1})[16] gives the product radical, $NAD^{\bullet}$. This slows the further increase in absorbance by formation of Comp I, with a lower molar absorptivity (ϵ = 35 mM^{-1} cm^{-1}) at 418 nm[11] as a result of the bimolecular reaction of Comp III with the product radical $NAD^{\bullet}$ (region *c* of Figure 2). One-electron reduction of Comp I forms Comp II (ϵ = 115 mM^{-1} cm^{-1} at 418 nm)[11] and further contributes to the increase in absorbance (region *d* of Figure 2).

Kinetic Model. As suggested above, the initial decrease in absorbance (region *a* of Figure 2) is the result of one-electron reduction of native HRP (Per^{3+}) to form ferroperoxidase (Per^{2+}). However, this reaction is too fast for quantitative treatment in the stopped-flow spectrophotometer used herein, and the rate constant has been excluded from the kinetic model for data fitting. Thus, in accordance with the above sequence of reactions (Figure 3), the increase in absorbance (regions *b*, *c*, and *d* of Figure 2) can be fitted to a kinetic model that assumes three sequential first-order pseudounimolecular reactions:

$$Per^{2+} \xrightarrow{k_1} \text{Comp III} \xrightarrow{k_2} \text{Comp I} \xrightarrow{k_3} \text{Comp II} \qquad (1)$$

This sequence of unimolecular reactions is described by the following system of ordinary differential equations:

$$\frac{d[Per^{2+}]}{dt} = -k_1[Per^{2+}] \qquad (2)$$

$$\frac{d[\text{Comp III}]}{dt} = k_1[Per^{2+}] - k_2[\text{Comp III}] \qquad (3)$$

$$\frac{d[\text{Comp I}]}{dt} = k_2[\text{Comp III}] - k_3[\text{Comp I}] \qquad (4)$$

$$\frac{d[\text{Comp II}]}{dt} = k_3[\text{Comp I}] \qquad (5)$$

For the purpose of fitting the kinetic trace (Figure 2), a solution of a system of ordinary differential equations 2, 3, and 4, with the amount of Comp II calculated from the mass−balance relationship, gives an analytical expression that describes the concentration of HRP intermediates in the enzyme-catalyzed oxidation of NADH:

$$[Per^{2+}] = [Per^{2+}]_0 \exp(-k_1 t) \qquad (6)$$

$$[\text{Comp III}] = \frac{[Per^{2+}]_0 k_1(\exp(-k_1 t) - \exp(-k_2 t))}{k_2 - k_1} \qquad (7)$$

$$[\text{Comp I}] = [Per^{2+}]_0 k_1 k_2 \left[\frac{\exp(-k_1 t)}{(k_2 - k_1)(k_3 - k_1)} + \frac{\exp(-k_2 t)}{(k_2 - k_1)(k_2 - k_3)} + \frac{\exp(-k_3 t)}{(k_3 - k_1)(k_3 - k_2)}\right] \qquad (8)$$

$$[\text{Comp II}] = [Per^{2+}]_0 - [\text{Comp I}] - [\text{Comp III}] - [Per^{2+}] \qquad (9)$$

Because the molar absorptivity of Comp I is ~3 times lower than the molar absorptivity of Comp III or Comp II at 418 nm and the molar absorptivity of Per^{2+} is about 2-fold lower than

(16) Fukuzumi, S.; Tanaka, T. In *Photoinduced Electron-Transfer Reactions, Part C. Photoinduced Electron-Transfer Reactions: Organic Substrates*; Fox, M. A., Chanon, M., Eds.; Elsevier: Amsterdam, 1988; Chapter 4.10.

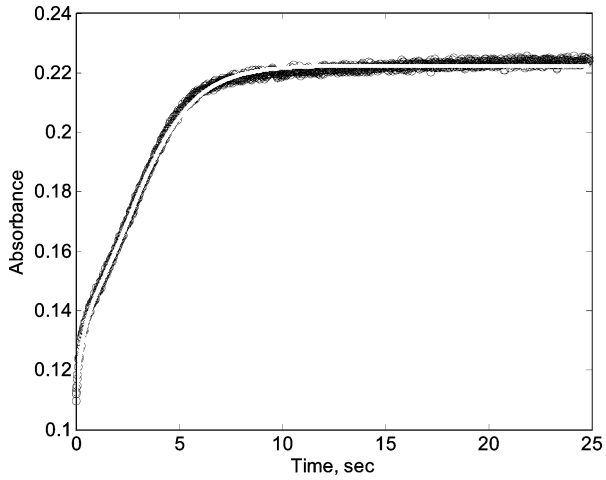

Figure 4. MatLab 6.5 for Windows fitting of the experimental data using eq 10. The extracted values of k_1, k_2, and k_3 (in s^{-1}) are the effective reaction rate constants: (○) experiment; (—) calculated fitting function.

Table 1. Magnetic-Field Dependence of the Rate Constants k_1, k_2, and k_3 on the HRP-Catalyzed Oxidation of NADH

gauss	$k_{1(H)}/k_{1(0)}$	$k_{2(H)}/k_{2(0)}$	$k_{3(H)}/k_{3(0)}$
0	1 ± 0.05	1 ± 0.05	1 ± 0.05
10	0.95 ± 0.05	0.90 ± 0.09	0.97 ± 0.06
30	0.83 ± 0.04	0.92 ± 0.07	0.95 ± 0.06
70	0.96 ± 0.05	1.1 ± 0.1	1.20 ± 0.07
100	0.93 ± 0.05	1.00 ± 0.08	1.00 ± 0.06
200	0.40 ± 0.02	0.98 ± 0.07	1.05 ± 0.06
600	0.80 ± 0.04	0.95 ± 0.07	1.1 ± 0.1
1000	1.14 ± 0.06	1.1 ± 0.1	1.1 ± 0.1
4000	0.63 ± 0.03	1.1 ± 0.1	0.80 ± 0.06

the molar absorptivity of Comp III or Comp II,[11,12] the final expression for fitting the experimentally determined change in absorbance at 418 nm can be written as follows:

$$A(418) = [\text{Comp III}] + [\text{Comp II}] + \frac{[\text{Comp I}]}{3} + \frac{[\text{Per}^{2+}]}{2} = [\text{Per}^{2+}]_0 - \frac{2[\text{Comp I}]}{3} - \frac{[\text{Per}^{2+}]}{2} \quad (10)$$

The Levenberg−Marquardt nonlinear least-squares fitting algorithm of Matlab 6.5 was used to fit the experimental data and to extract values for k_1, k_2, and k_3. Figure 4 shows good agreement between an experimental kinetic trace and the corresponding fitted function (10).

Magnetic-Field Dependence. Stopped-flow kinetic traces of the HRP-catalyzed oxidation of NADH were collected in a random order of magnetic-field strengths ranging from 0 to 4000 G. Each kinetic trace was fitted to eq 10, and the values for k_1, k_2, and k_3 were extracted (Table 1). Only the first effective rate constant k_1 (the rate constant for conversion of ferroperoxidase Per^{2+} to Comp III, as specified in eq 1) was found to be magnetic-field sensitive, while rate constants k_2 and k_3 do not exhibit any magnetic-field dependence. Figure 5 shows the magnetic-field effect (MFE) on rate constant k_1, that is calculated as the ratio of the rate constant at nonzero magnetic field $k_{1(H)}$ relative to the same rate constant at zero magnetic field $k_{1(0)}$. A sharp decrease in the value of k_1 is observed at 200 G, and a steep increase in k_1 is observed from 200 to 1000 G, followed by a smaller decrease from 1000 to 4000 G.

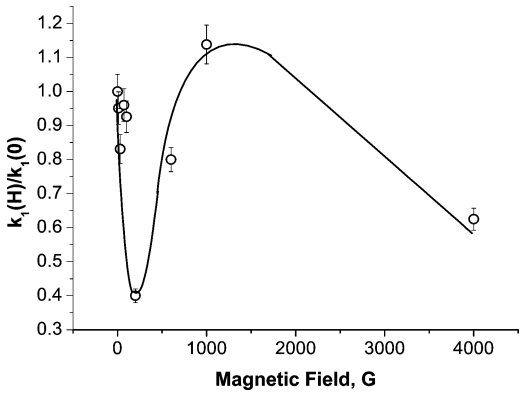

Figure 5. Magnetic-field effect on the rate constant k_1 of the NADH oxidation catalyzed by HRP. Kinetic traces at 418 nm were fitted to the model described by eq 1. Error bars show the sum of 3.5% deviation of the instrumental mean error and standard deviation after the averaging of three experimental series each with 5−6 measurements at each magnetic-field strength. Reaction conditions (all concentrations after mixing): 100 mM MES; pH = 5.56; [HRP] = 1.0 μM; [NADH] = 100 μM; 25.0 °C.

The magnetic-field dependence of k_1 can be interpreted within the theoretical framework of magnetic-field dependent radical pair recombination. According to MFE theory,[13] the magnetic-field dependence of a reaction can arise from a pair of paramagnetic species (or radicals) that exist in a single magneto-sensitive intermediate of the enzyme-catalyzed reaction. The catalytic cycle of HRP is known to involve a number of paramagnetic species,[9,14,17] including native HRP with Fe^{3+} at the catalytic site, ferroperoxidase Per^{2+} with Fe^{2+} at the catalytic site, and three iron−oxo Fe^{IV}═O intermediates (Comp I, Comp II, and Comp III), as well as paramagnetic O_2 and an organic product radical that is derived from the substrate (see also Figure 3). However, it is reasonable to assume that because only k_1 demonstrates an experimentally observed dependence on an external magnetic field, the MFE shown in Figure 5 might arise at the first stage of the oxidation process, that is, the single-electron-transfer step involving ferroperoxidase Per^{2+} and the $NADH^{\bullet+}$ radical cation.

Analysis of MFEs and Theoretical Modeling of the Multispin Paramagnetic Pair. Single-electron transfer from NADH to native HRP produces the quartet radical pair (Q) of Per^{2+} and the $NADH^{\bullet+}$ radical cation that is unreactive toward recombination (Figure 6). Intersystem crossing converts the quartet (Q) to the doublet electron-spin state (D), and the pair can then undergo recombination to regenerate native HRP and NADH. Escape of intermediates from the cage can occur from both the quartet and doublet electron-spin states to enable forward reaction progress. Two characteristic features of this reaction in condensed media can be traced to a "cage effect", a comparatively long contact encounter of the radical pair or a pair of paramagnetic species and the possibility of re-encounter resulting from radical diffusion. To allow for all re-encounters of the (Per^{2+}−$NADH^{\bullet+}$) paramagnetic pair, the theoretical recombination probability has been calculated in the framework of a two-position model that is a particular case of the density matrix formalism.[18] The observed quartet−doublet spin evolution of the paramagnetic pair (Figure 6) is defined by the electron-spin interaction with the external magnetic field, the

(17) Frew, J. E.; Jones, P. In *Advances in Inorganic and Bioinorganic Mechanisms*; Sykes, G., Ed.; Academic Press: New York, 1984; p 175.
(18) Purtov, P. A.; Doktorov, A. B. *Chem. Phys.* **1993**, *178*, 47−65.

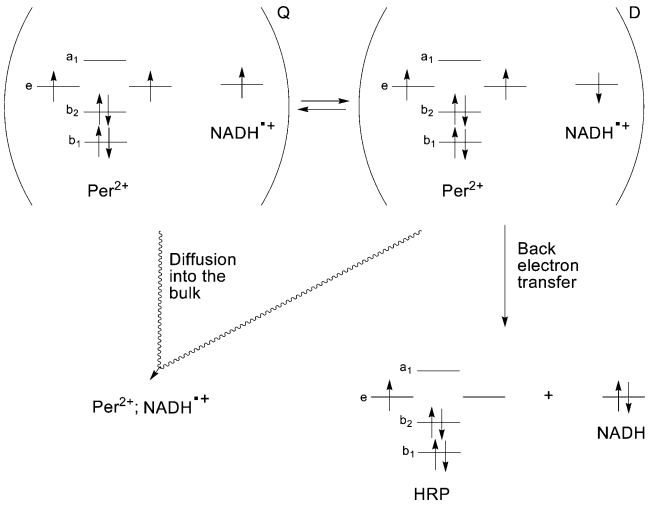

Figure 6. Spin evolution in the Per^{2+} and $NADH^{\bullet+}$. The Q and D pairs are the quartet and doublet spin states of the paramagnetic pair $(Per^{2+}\ NADH^{\bullet+})^{Q,D}$. The electronic structures of the ferroperoxidase Per^{2+} and HRP are drawn on the basis of the splitting in the distorted tetrahedral crystal field (see also corresponding structures in Figure 2).

isotropic hyperfine interaction of the unpaired electrons with magnetic nuclei in the system, and the electron-exchange interaction that splits the energy terms of the paramagnetic pair into the doublet and quartet spin states. Hence, the Hamiltonian for the system can be written as follows:

$$\hat{H} = \omega_1\hat{S}_1 + \omega_2\hat{S}_2 + a\hat{S}_2 I + J\hat{S}_1\hat{S}_2 \qquad (11)$$

where $\omega_1 = g_1\beta h^{-1}H_0$ and $\omega_2 = g_2\beta h^{-1}H_0$ are the Larmor precession frequencies of the paramagnetic particles comprising the pair ($Per^{2+}\ NADH^{\bullet+}$) in the magnetic field H_0; a is the effective constant of isotropic hyperfine interaction between the unpaired electrons of $NADH^{\bullet+}$ with a magnetic nucleus of spin equal to $^1/_2$ for the radical cation; and J is the exchange integral between the doublet and quartet terms of the paramagnetic pair. In general, the exchange interaction magnitude depends on the distance between the paramagnetic species as well as on the orientation angles, that is, $J(r,\theta,\varphi)$. However, accounting for all of these factors complicates the calculations tremendously. Therefore, the present work considers only two possible conformations of the pair ($Per^{2+}\ NADH^{\bullet+}$) with two corresponding exchange integrals $J_1 = 200 \times 10^7$ rad/s and $J_2 = 265 \times 10^7$ rad/s. The value of the exchange integrals are varied parameters in the calculated magnetic-field dependence and are well within the expected range for exchange interactions in bound radical ion pairs. A calculation of the magnetic-field dependence also requires the magnetic-resonance parameters of the paramagnetic species that form a pair with magnetic-field dependent spin evolution (e.g., effective hyperfine interaction and radical g-factors). ESR studies of HRP show that divalent iron complexes with a structure similar to the ferroperoxidase Per^{2+} catalytic site have g-values close to 3.2,[19] and $NADH^{\bullet+}$ has a g-value equal to 2.0032, with an effective hyperfine interaction of about 33 G.[20] Figure 7 shows the magnetic-field dependence of the recombination probability of the quartet pair

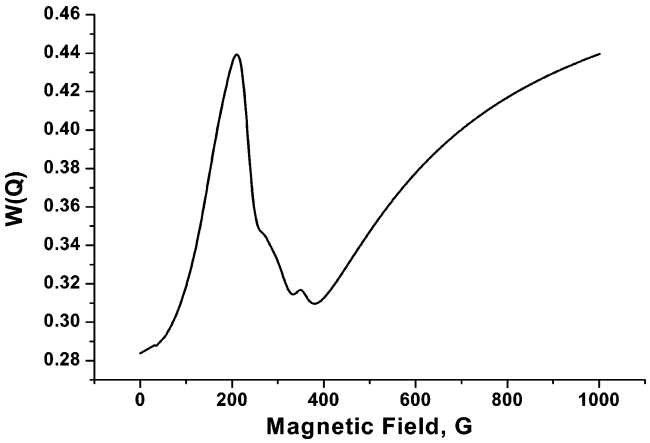

Figure 7. Theoretical modeling of the recombination probability of the quartet radical pair $(Per^{2+}\ NADH^{\bullet+})^{Q}$ magnetic-field dependence.

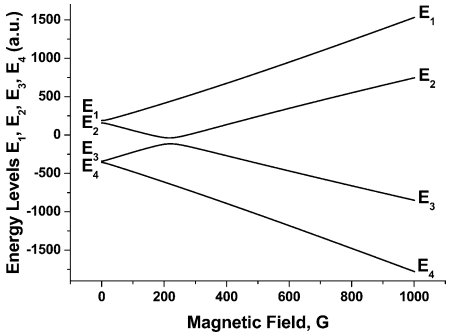

Figure 8. Q−D transitions in the paramagnetic pair $(Per^{2+}\ NADH^{\bullet+})^{Q}$. Splitting of the stationary energy levels in the external magnetic field (for the total spin projection equal to 0).

$(Per^{2+}\ NADH^{\bullet+})^{Q}$, W(Q), calculated in the framework of the two-position model described above.

The above Hamiltonian of the system under study (11) commutates with the projection of the total spin of the electrons and nucleus onto the direction of the external magnetic field, with the total projection being equal to:

$$\hat{\Sigma}_Z = \hat{S}_{1Z} + \hat{S}_{2Z} + \hat{S}_Z \qquad (12)$$

Because only the states with the same total projections participate in quantum transitions, then all spin states of the paramagnetic pair could be divided into the following subensembles: $\Sigma_Z = \pm 2$, $\Sigma_Z = \pm 1$, and $\Sigma_Z = 0$, while the states with only the total projection equal to $+1$, -1, and 0 contribute to recombination. Figures 8 and 9 show the behavior of the stationary energy levels of the above-mentioned subensembles that is obtained through the solution of the Schrödinger equation with Hamiltonian (11). The level crossing evident in the range of 200−250 G suggests that the dependence of the recombination probability should demonstrate an extreme point exactly in this region of an external magnetic field.

The probability of residence of a radical pair in the recombinant singlet state at any moment follows the law:[21]

$$\rho_{SS}(t) = \sum_i |c_i|^4 + \sum_{i,j} |c_i|^2 \cdot |c_j|^2 \cos((E_i - E_j)\hbar^{-1}t) \qquad (13)$$

where E_i are Eigenvalues of a radical pair Hamiltonian, $c_i \equiv$

(19) Pavel, E. G.; Kitajima, N.; Solomon, E. I. *J. Am. Chem. Soc.* **1998**, *120*, 3949−3962.
(20) Hore, P. J.; Volbeda, A.; Dijkstra, K.; Kaptein, R. *J. Am. Chem. Soc.* **1982**, *104*, 6262−6267.
(21) Sukhenko, S. A.; Purtov, P. A.; Salikhov, K. M. *Khim. Fiz.* **1983**, *1*, 21−27.

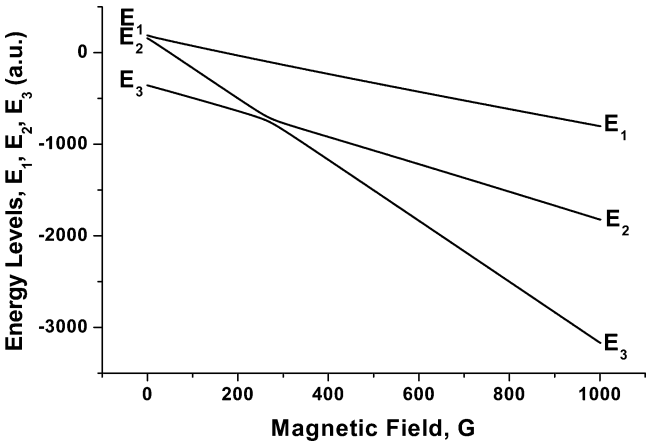

Figure 9. Q−D transitions in the paramagnetic pair $(Per^{2+}\ NADH^{\bullet+})^{Q}$. Splitting of the stationary energy levels in the external magnetic field (for the total spin projection equal to −1).

$\langle i|S\rangle$ are expansion coefficients of the singlet state wave function $|S\rangle$ to Eigenfunctions $|i\rangle$ of a Hamiltonian. After time averaging a field dependence of the singlet state population, eq 13 is transformed into:

$$\overline{\rho_{SS}}(H) = \sum_i |c_i|^4 + 2|c_n|^2 \cdot |c_k|^2 \delta(H,H^*) \qquad (14)$$

where delta-function $\delta(H,H^*) = 0$ for nondegenerated energy levels and $\delta(H,H^*) = 1$ in the degenerate case.

Zeeman energy splitting is absent at zero magnetic field, therefore, the energy levels of the paramagnetic pair are degenerate (Figure 10, (1)). Equation 14 shows that in the range where the energy levels are degenerate, the efficiency of singlet−triplet (S−T) mixing decreases. Thus, by analogy, the mixing of doublet−quartet (D−Q) transitions with recombinant D- and nonrecombinant Q-states decreases. Thus, at zero magnetic field, the maximum recombination probability is attained for a paramagnetic pair formed in the D-state, while the Q-born pair will show minimal recombination probability. This is consistent with the observation that a minimum value of the recombination probability W(Q) occurs at zero magnetic field (Figure 7). With an increase of the external magnetic field, the degeneracy of the energy levels is removed, and this results in the gradual increase of the recombination probability W(Q). Figures 8 and 9 show that the stationary energy levels of the pair $(Per^{2+}\ NADH^{\bullet+})$ for the subensembles contributing to recombination cross again in the magnetic-field range from 200 to 250 G. At this magnetic-field strength, the efficiency of Q−D transitions reaches a maximum value, because Q−D mixing is maximal in the fields equal to

$$H_0 = \frac{3J}{2(g_1 + g_2)\beta} \qquad (15)$$

where J is the exchange integral; g_1 and g_2 are g-values of Per^{2+} and $NADH^{\bullet+}$, respectively; and β is the Bohr magneton (Figure 10, (2)). At magnetic fields higher than the local maximum at about 200 G, Zeeman interactions lead to a further splitting of energy levels (Figure 10, (3)), therefore, the Q−D transitions decrease and the recombination probability decreases W(Q) (Figure 7). Because the frequency of transitions in higher magnetic fields is determined by the difference in the Larmor precession frequencies of a radical pair, an increase of the external magnetic field above 400 G results in a more frequent occurrence of Q−D transitions, thus leading to the growth of W(Q) (Figure 7) in the magnetic-field range from 400 to 1000 G.

Theoretical calculations of the recombination probability W(Q) (Figure 7) show the influence of an external magnetic field on the Q−D transitions in the paramagnetic pair $(Per^{2+}\ NADH^{\bullet+})^{Q}$. Recombination of the pair results in the regeneration of native HRP (see Figure 6). Therefore, the influence of an external magnetic field on the formation of Comp III as a result of the bimolecular reaction between Per^{2+} and dissolved oxygen (Figure 3) is described by the escape probability $(1 - W(Q))$; Figure 11), which models the experimentally observed dependence of the rate constant k_1 on the applied magnetic field (Figure 5). Thus, excellent agreement between the experimentally observed magnetic-field dependence and the calculated recombination probability (including the approximate size of the magnetic-field dependence and the location of the inflection extremes) strongly support the proposed interpretation of the magnetic-field dependence of HRP.

Conclusions

The kinetic description of the HRP-catalyzed oxidation of NADH, as well as the influence of an external magnetic field on the electron-spin transformation of active HRP intermediates of the catalytic cycle of NADH oxidation has led to a new understanding of the elementary reaction steps of HRP with NADH. Analysis of the kinetic traces suggests that in the absence of H_2O_2 the following transformations best describe the HRP-catalyzed oxidation of NADH:

$$Per^{2+} \xrightarrow{O_2} \text{Comp III} \xrightarrow{NAD^{\bullet}} \text{Comp I} \xrightarrow{NADH} \text{Comp II} \qquad (16)$$

It is assumed that ferroperoxidase, Per^{2+}, is formed through single-electron transfer from NADH to native HRP (eq 17). This model is consistent with the experimentally observed magnetic-field dependence of the reaction (Figure 5), when compared to the corresponding theoretical calculations (Figure 11).

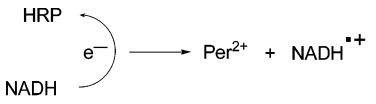

(17)

This new suggestion for the first stage of NADH oxidation is quite uncommon, because it was believed that Per^{2+} is generated only in a side reaction of the HRP catalytic cycle (Figure 1b). Of special interest is evidence for the involvement of $NADH^{\bullet+}$ radical cation in the enzymatic oxidation. A continuum of the reaction mechanisms from discrete hydride transfer at one mechanistic extreme to the asynchronous ECE ("electron−chemical−electron") reaction at the other mechanistic extreme is possible. The magnetic-field dependence of enzymatic reaction kinetics and the analysis of electron-spin dependent product distributions offer unique tools to study the mechanism of enzymatic reactions that incorporate paramagnetic pair intermediates. The techniques of electron-spin chemistry offer the possibility to identify kinetically relevant and short-lived paramagnetic intermediates in biologically relevant processes. It is worth noting that the involvement of radical ions and neutral radicals in model redox reactions of NADH and its

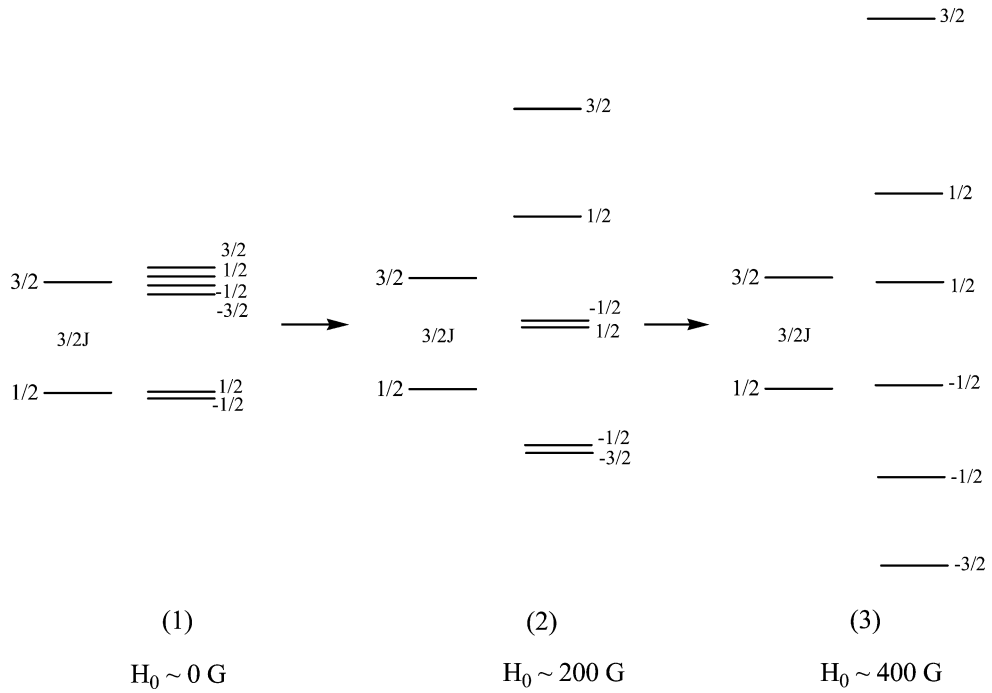

Figure 10. Splitting of energy terms of the paramagnetic pair (Per^{2+} $NADH^{\bullet+}$) with increasing external magnetic-field strength.

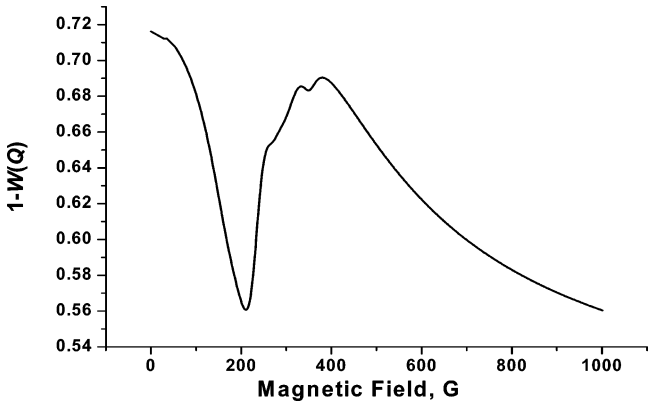

Figure 11. Dependence of the calculated escape probability ($1 - W(Q)$) for the paramagnetic pair (Per^{2+} $NADH^{\bullet+}$)^Q on the external magnetic-field strength, as modeled by the experimentally observed magnetic-field dependence of the rate constant k_1.

synthetic analogues was demonstrated previously by means of another spin chemistry technique, CIDNP.[20,22]

Analysis of the magnetic-field dependence of the HRP-catalyzed oxidation of NADH and comparison to theoretical modeling of the electron-spin dependence of the reaction of enzyme intermediates strongly suggests that single-electron transfer from NADH to native HRP is the first step of the catalytic pathway in the absence of H_2O_2. In this regard, only inclusion of the significant electron-exchange interaction in the paramagnetic pair (Per^{2+} $NADH^{\bullet+}$) in the model calculations allowed a determination of the expected minima and maxima of the values for rate constant k_1 as a function of magnetic field (Figures 5 and 11) near 200 G. The existence of an extreme minimum and maximum effect within a narrow range of magnetic-field strength suggests that the partners of the above pair are bound in an enzyme−substrate complex and that electron transfer is not merely the product of "hit-and-run" electron transfer from NADH to the edge of the heme cofactor.

In addition, influence of the external magnetic field on the effective rate constants for the interconversion of reactive species in the catalytic cycle of HRP indicates an absolute requirement for the correct electron-spin state to allow the reaction to proceed. The doublet state of the paramagnetic pair can undergo recombination to regenerate native HRP, while in accordance with the electron-spin-state selection rules, the quartet state channels of ferroperoxidase Per^{2+} do not undergo nonproductive recombination, but lead to forward catalytic throughput in the cycle (Figure 6). Thus, an external magnetic field is able to accelerate or decelerate enzymatic catalysis by altering the frequency of nonproductive recombination, as determined by the electron-spin multiplicity of the initial paramagnetic pair. To predict the magnetic-field dependence of an enzymatic reaction qualitatively and quantitatively, one must consider the electron-spin multiplicity of any paramagnetic intermediates and apply the Wigner electron-spin conservation rule that states the electron-spin multiplicity must remain unchanged in an elementary electron-transfer step.

The present paper is not the first report of the influence of electron-spin state on reactive intermediates in an enzyme-catalyzed reaction.[14,23] However, the present report is the first example of the application of radical pair theory for the description of electron-spin evolution in a paramagnetic pair with more than two unpaired electrons. Furthermore, this approach suggests a pathway that begins with single-electron transfer to activate native HRP in the absence of H_2O_2 as the initial oxidant.

Experimental Section

Reagents. HRP was purchased from Sigma, Inc. (type XII, 250−330 U/mg, R/Z > 3.1), and used without further purification. The final concentration of the enzyme was 1.0 μM after mixing. The enzyme

(22) Taraban, M. B.; Kruppa, A. I.; Polyakov, N. E.; Leshina, T. V.; Lusis, V.; Muceniece, D.; Duburs, G. *J. Photochem. Photobiol., A* **1993**, *73*, 151−156.

(23) Harkins, T. T.; Grissom, C. B. *J. Am. Chem. Soc.* **1995**, *117*, 566−568.

concentration was determined spectrophotometrically using a molar extinction coefficient of 102 mM^{-1} cm^{-1} at 403 nm. β-NADH was purchased from U.S. Biochemical, and the final concentration after mixing was 100 μM. The concentration of NADH was determined spectrophotometrically using a molar extinction coefficient of 6220 M^{-1} cm^{-1} at 340 nm. All experiments were carried out in 100 mM MES buffer at pH 5.56. All solutions except MES buffer were prepared fresh daily. All solutions were passed through a 0.45 μm filter prior to use.

Stopped-Flow Kinetic Experiments. Pre-steady-state kinetic experiments were carried out with a rapid-scanning stopped-flow spectrophotometer (OLIS−RSM) that can record a full absorbance spectrum at 1 kHz. The instrument has a mixing dead-time of 1.3 ms, as determined with dichloroindophenol and ascorbate. A circulating water bath maintains the temperature of the drive syringes and reaction cuvette (1.7 cm optical path) at 25 °C. The OLIS−RSM was modified to position the reaction cuvette in the air gap of an electromagnet that produces an adjustable magnetic field in the range of 0 to 4500 G.[23] Absorbance spectra were recorded from 310 to 600 nm at a sampling rate of 1 kHz. Prior to mixing, equal amounts of enzyme and substrate solutions were kept in separate syringes. The output from the spectrophotometer was recorded over at least 45 s at a sampling rate of 62 scans/s (digitally averaging 16 scans per measurement). Kinetic traces were extracted by digitally selecting the change in absorbance at 418 nm. The magnetic-field strength was varied from 10 to 4000 G. Before recording data for each stopped-flow shot at a nonzero magnetic-field value, a stopped-flow shot at 0 G was recorded as a control. Zero gauss is defined as 0 G of the applied laboratory magnetic field, as recorded on a Hall sensor placed in the gap of the electromagnet but not corrected for the off-axis geomagnetic-field component that is approximately 0.3 G in Utah. Kinetic data from the spectrophotometer were stored on disk for later analysis.

Acknowledgment. This work has been supported by grants from the U.S. Civil Research and Development Foundation (RC2-2390-NO-02) and the Russian Foundation for Basic Research (04-03-32277).

JA0585735